Towards time-reduced cure cycles of epoxy resins for mass production of composites maintaining the thermo-mechanical properties.

José Antonio González[1,2], Jordi Farjas[3*], Norbert Blanco[1], Josep Costa[1], Marc Gascons[2] and Daniel Sánchez-Rodríguez[3]

[1]AMADE - Analysis and Advanced Materials for Structural Design, Universitat de Girona, Campus Montlivi, Edif. PII, Girona, E-17003, Catalonia, Spain.
[2]COMPOXI, C/Pic de Peguera 9, Technological and Scientific Park of the University of Girona, Girona, E-17003, Catalonia, Spain.
[3*]GRMT - Materials Research Group and Thermodynamics, Universitat de Girona, Campus Montlivi, Edif. PII, Girona, E-17003, Catalonia, Spain.

*Corresponding author(s). E-mail(s): jordi.farjas@udg.edu;

Abstract

Because long curing times hinder the mass manufacturing of composite products, there is a constant quest to develop shorter curing cycles that maintain material quality. The authors recently developed a curing prediction methodology for thermoset composites based on an isoconversional model, which is used in this work to shorten the curing time of real practice processes. The investigation presents two optimized cure cycles devised to reduce the curing times recommended by the resin manufacturer while assure a complete degree of cure and restricting the exothermal flow to avoid undesired overheating. The mechanical (compression, in-plane and interlaminar shear) and physical ($\boldsymbol{T_g}$, void content, outgassing) properties of specimens extracted from panels manufactured according to recommended curing cycles and the two time-reduced cycles

(up to 72% shorter) presented here, exhibited deviations of less than 4% and always fell within the acceptable range for the most demanding of industrial sectors: aeronautics. The results support the prediction model's feasibility to achieve more efficient and productive processes.

Keywords: Time-reduced curing cycle, thermo-mechanical properties, VTC401 epoxy, composites manufacturing, autoclave cure

1 Introduction

Manufacturers of resins and derived products, for instance, carbon-epoxy prepregs, provide manufacturing procedures consisting of time-temperature histories (recommended cure cycles) that have been devised to guarantee good quality; irrespective of a part's geometry [1, 2]. To do so, they adopt conservative curing profiles involving long run times. Consequently, while the composite industry is particularly interested in shortening the curing processes, they need to ensure the thermomechanical properties of the resulting component [3, 4]. Inadequate curing profiles can result in temperature overshoots, under- or over-curing, side reactions, or non-uniform degrees of curing within the composite parts [5–7].

Extensive research has been conducted into reducing cure cycles but that, nonetheless, ensures the quality of the processed composite material. Tang et al. [8] recently proposed a multi-objective optimization method mainly based on thermo-kinetic coupled simulations to optimize curing profiles for autoclave processed composites. The cure kinetics were implemented using a model-fitting model, whilst also considering the heat transfer and thermal conductivities of the composite. Compared to the typical cycle for a 3501-6 resin system, the total curing time was reduced by 19% and still maintained mechanical performance. Dolkun et al. [9] applied a similar thermo-kinetic approach but, in this case, employed a multi-objective genetic algorithm and the Pareto optimal front. The researchers found a 33% reduction in the total cure time for a 24-mm thick unidirectional laminate made of RTM6 epoxy resin and managed to prevent thermal detrimental effects. Yuan et al. [10] proposed a surrogate model based on the Surface Response Method oriented to cure optimization of composite laminates. Accordingly, they considered heat transfer, cure kinetics (model-fitting), and resin flow-compaction in the prediction approach and were able to achieve a 45%-time-reduction for the epoxy resin system 3501-6.

Those studies required an extensive number of thermo-chemical parameters to power the cure degree prediction methods, which also entailed complete test campaigns. In fact, established resins (i.e., 3501-6, RTM6 or 8552), which are supported by extensive literature, are commonly used to validate new prediction methods [11–13] but as they require complete experimental testing,

this poses a barrier to the process optimization of novel or not-so-common resins.

Besides, isoconversional methods allow to easily characterize the kinetics of the curing process [14–23]. The reason is that isoconversional methods are model-free, i.e., they do not assume any type of mechanism. Therefore, their application can be extended to different types of resins without having to determine the particular mechanisms involved in the curing process of a given resin. In a recent contribution we have demonstrated the ability of isoconversional methods to predict the degree of cure of epoxy-based composites under complex thermal histories [24]. First, the kinetic parameters of VTC401 and M18 epoxy resins were determined using isoconversional methods, and then the predictions for the cure processes were validated in the laboratory through mixed dynamic and isothermal DSC experiments. Because predictions can be made for an arbitrary temperature program, is especially suited to dealing with industrial processes, paving the way to optimizing the curing cycles of epoxy resins, shortening run times and, consequently, improving productivity.

In this manuscript, the kinetic approach developed in [24] is used to reduce the cure cycle time of the VTC401 epoxy resin in a real manufacturing environment in the composite industry. As the approach presented does not consider heat transfer or thermal conductivity throughout the composite part, this work will not describe the heat generated by the exotherm reaction or transported across the sample.

The present research compares the thermo-mechanical and physical properties of 2 mm-thick carbon-epoxy VTC401 panels cured following the manufacturer's recommended cure cycle (MRCC), with the results from two optimized cycles: cure Cycle 1, aimed at shortening the curing time while maintaining the heating and cooling ramps specified by the manufacturer, and cure Cycle 2, which alters the ramps and dwell times to achieve full curing in the minimum time while controlling the heating rate to avoid a harmful exothermal flow.

The results show that, with respect to MRCC for VTC401 epoxy resin, curing times for Cycles 1 and 2 are optimized by 38% and 72% while still guaranteeing the highest mechanical and thermal properties of the material. Thus, the proposed approach can lead to increased productivity in composite manufacturing.

2 Methodology

2.1 Kinetic methods

Isoconversional methods are based on the assumption that the rate of transformation at a given degree of transformation, α depends only on the temperature and the degree of transformation [25–27]:

$$\left[\frac{d\ln(d\alpha/dt)}{dT^{-1}}\right]_{\alpha} = -\frac{E_{\alpha}}{R_G}, \tag{1}$$

where t is time, T is the temperature and E_α is the apparent activation energy at a particular α and R_G is the universal gas constant.

The equation governing the kinetics can be obtained from the integration of Equation 1:

$$\frac{d\alpha}{dt} = Af(\alpha)e^{-\frac{E_\alpha}{R_G T}} \tag{2}$$

where A is a preexponential term and $f(\alpha)$ is a function related to the reaction model. Hence, the kinetics is fully described by the apparent activation energy, E_α and the term $Af(\alpha)$. Note that both parameters depend on the degree of transformation α.

Differential isoconversional methods are based on the determination of the temperature $T_{j,i}$ and transformation rate $\left(\frac{d\alpha}{dt}\right)_{j,i}$ for a given degree of transformation α_j and different thermal histories identified by the subscript i. Specifically, to determine the degree of transformation we have performed differential scanning calorimetry measurements at five different heating rates, β_i. These experiments are reported in [24].

Friedman isoconversional method is derived directly from Equation 2:

$$ln\left(\frac{d\alpha}{dt}\right)_{j,i} = -\frac{E_j}{R_G T_{j,i}} + ln\left(Af(\alpha)\right)\big|_j, \tag{3}$$

according to Equation 3 for a given degree of transformation, α_j, a plot of $ln\left(\frac{d\alpha}{dt}\right)_{j,i}$ with respect $1/T_{j,i}$ should result in a straight line. From the slope and y-intercept we obtained E_j and $\left(Af(\alpha)\right)\big|_j$ respectively, where E_j is E_α for $\alpha = \alpha_j$.

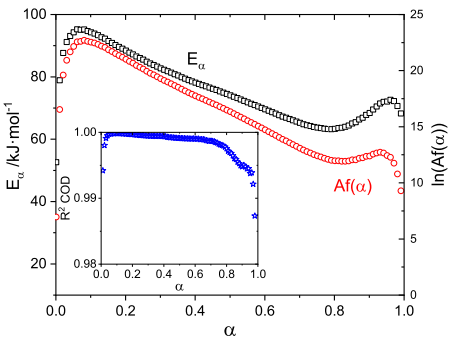

Fig. 1 Result of Friedman isoconversional analysis: E_α (Black squares) and $Af(\alpha)$ (red ciercles). The units of $Af(\alpha)$ are s^{-1}. Inset: The R^2 coefficient of determination of the Friedman linear fit.

Figure 1 shows the result of Friedman isoconverisonal analysis. The coefficient of determination R^2 of the linear Friedman fit is very close to one, which confirms that the isoconversional principle is fulfilled for the temperature range analysed. As for the discretisation of the degree of transformation,

we have taken $\Delta\alpha = 0.001$ so that $0 \leq j \leq 1001$. For the sake of clarity, only one out of ten data points has been plotted in Figure 1.

Once the kinetic parameters have been obtained, we can predict the evolution of the reaction when the temperature is constant or when it rises at constant rate [16–18, 22, 28–31]. The method developed in refs. [32, 33] allows to predict the evolution of the cure reaction for an arbitrary temperature program, $T(t)$. This method is based on the summation of Equation 2 over small time intervals Δt:

$$\alpha_{k+1} = \alpha_k + Af(\alpha)|_k \exp\left(-\frac{E_k}{R_G T_k}\right)\Delta t_k. \tag{4}$$

where $T_k = T(t_k)$ is the discretization of the temperature history, Δt_k is the time interval between T_k and T_{k+1}, α_k, E_k and $Af(\alpha)|_k$ are α, E_α and $Af(\alpha)$ when $\alpha = \alpha_k$. These parameters are obtained directly from the interpolation of the kinetic parameters provided by the Friedman analysis. To improve the accuracy we performed a cubic spline interpolation.

Therefore, the evolution of the transformation degree is obtained by iterating k starting with the initial condition $\alpha_0 = 0$. Equation 4 is obtained by substituting the differential terms in Equation 2 by finite differences. Thus, to obtain a reliable prediction it is mandatory to use a small time step, so that during a time step the activation energy and $Af(\alpha)$ are approximately constant. Otherwise, the approximation of replacing differential terms by finite differences will be quite inaccurate. In our predictions we have taken a time step of one second.

Finally, it is important to note that the kinetic parameters have been obtained from experiments carried out at constant heating rate up to temperatures well above the maximum glass transition temperature. Under these conditions, vitrification occurs when the sample is fully cured. Therefore, the kinetic predictions do not take vitrification into account.

2.2 Experimental

To reduce the cure cycle time of a 2 mm thick carbon reinforced polymer (CFRP) with VTC401 (SHD Composite Materials Ltd) epoxy resin, we used the kinetic methods introduced in the previous subsection to define two new cure cycles (Cycles **1** and **2**). First, we have determined the kinetic parameters (E_α and $Af(\alpha)$) as a function of the degree of curing, see Figure 1. Next, a temperature-time profile (any desired profile customised in any way) is the only input needed to make predictions, which are performed using Equation 4.

The VTC401 epoxy resin system was chosen because it cures faster than other resins with similar mechanical properties, largely due to its diamine content [24]. The MRCC consists of a ramp-up to 120°C at 2°C min^{-1}, a 45 minute dwell at 120°C, a second ramp-up to 135°C at 0.3°C min^{-1}, then a second dwell at 135°C for 2 hours and, finally, a cooling down at 2°C min^{-1} (Figure 2), for a total time of 325 minutes.

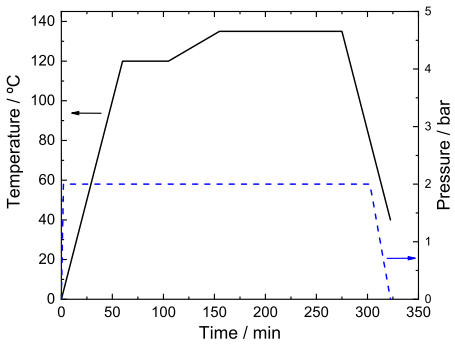

Fig. 2 Manufacturer's Recommended Cure Cycle (MRCC) for the VTC401 epoxy resin (SHD Composite Materials Ltd) [2].

Cure Cycle **1** was tailored to minimize the temperature dwell time while guaranteeing complete curing of the 2 mm thick laminate, maintaining the same heating ramps and temperature boundaries as specified in the MRCC. First, we experimentally recorded the temperature evolution of a laminate subjected to the MRCC cycle. To confirm that there were no significant temperature gradients across the thickness, we used 11 thermocouples located between plies (Figure 3). Then, with Equation 4, we have calculated the evolution of the degree of cure using the experimentally recorded thermal history. Finally, the onset of the cooling ramp for the optimized cure Cycle **1** was set as the time at which the prediction indicates that the maximum degree of cure has been reached.

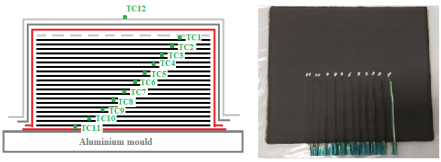

Fig. 3 Left: embedded thermocouples scheme. Right: manufactured CFRP panel. Thermocouples are placed in numerical order from right (1) to left (11).

Cure Cycle **2** aims to reach a complete degree of cure in the shortest possible time while controlling the maximum transformation rate, $d\alpha/dt$. In this case, the curing prediction is not based on a measured thermal evolution, but an imposed theoretical temperature program that fulfills the stated objectives.

Both optimized cure cycles were conceived to reach the maximum degree of cure according to the kinetic model. Therefore, if the prediction method is valid, the thermo-mechanical properties of the laminates, irrespective of the cure cycle (MRCC, **1** or **2**), should be similar. To validate this hypothesis, experimental tests were carried out comparing different mechanical and physical properties of the manufactured panels.

The experimental mechanical evaluation focused on matrix-dependent properties to detect a hypothetical variation in the final state of the resin, depending on the curing cycle [34, 35]: the interlaminar shear strength (ILSS), compression and in-plane shear strength (IPSS) tests. The physical properties of the matrix measured were glass transition temperatures (T_g), loss of volatiles (through the total mass loss) and void content (% VC), properties known to be very dependent on the degree of cure.

The test matrix in Table 1 was applied to specimens in each cure cycle. According to testing standards (Table 1), specimens were 2 mm thick to maintain reasonable in-plane dimensions. The stacking sequence is also defined by the corresponding standard.

Table 1 Test matrix for the MRCC and cure cycles 1 and 2 (*does not apply to cure cycle 2).

Test type	Standard	Property	N° specimens	Stacking sequence	Specimen (mm^3)
Interlaminar Shear Strength (ILSS)	ISO 14130	Interlaminar shear strength	5	$[0°]_{20}$	$20 \times 10 \times 2$
Compression Strength, 0°	ASTM D6641	Compression strength	5*	$[0°]_{20}$	$140 \times 13 \times 2$
In-Plane Shear Strength (IPS)	EN 6031	In-plane shear strength	5*	$[+45/\text{-}45]_{5s}$	$230 \times 25 \times 2$
Differential Scanning Calorimetry (DSC)	EN 6041	Glass transition temperature (T_g)	2	$[0°]_{20}$	$20 \times 10 \times 2$
Outgassing	Internal procedure	Total mass loss (TML)	2	$[0°]_{20}$	$20 \times 10 \times 2$
Fibre Volume Fraction (FVF)	EN 2564	% FVF	2	$[0°]_{20}$	$20 \times 10 \times 2$
Void Content (VC)	EN 2564	% VC	2	$[0°]_{20}$	$20 \times 10 \times 2$

The composite laminates were manufactured using M55J/VTC401 carbon epoxy unidirectional prepreg (SHD Composite Materials Ltd) of 100 g m^{-2} areal weight and 32% resin weight content [2].

The dimensions of the panels were $300 \times 300 \times 2$ mm^3. As two different stacking sequences are needed to manufacture the specimens in the test matrix, two different panels were laminated per each of the curing cycles. In addition to these six panels, another was manufactured earlier with embedded thermocouples (Figure 3) to measure the temperature – time (T–t) evolution during MRCC. The thermocouples were placed every two layers and staggered to cover a greater surface.

The panels were laminated using a prepreg hand lay-up and subsequently cured in a conventional autoclave system (Figure 4). An aluminium mould was covered with polyolefin non-perforated release film. Prepreg layers were cut to size and placed on the mould according to the laminate stacking sequence. A standard peel-ply was then placed on top of the laminate, and a teflon-coated glass fabric was used as an edge breather to remove entrapped air from the laminate stack. A commercial breather was used for an even distribution of vacuum. The entire setup was sealed using a vacuum bag with bagging tape.

The vacuum pressure was 0.95 bar. Debulking was performed after the first layer and then every three layers (duration of 5 min), to remove trapped air from within the laminate stack and ensure good prepreg compaction. Figure 4 shows the bagging scheme. The same configuration was used for all panels.

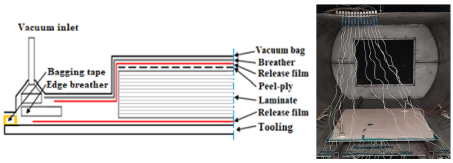

Fig. 4 Left: vacuum bagging scheme of the manufactured panels. Right: autoclave setup ready to cure a batch of CFRP panels.

ILSS tests were carried out according to ISO14130 standards at room temperature using a 5 kN MTS Insight electromechanical machine to assess not only any variation in the matrix but the resulting interlaminar resistance. Load was measured with a 5 kN load cell working at 100% of its range. The span length was 10.33 mm, the diameter of the supports was 4 mm, and the loading nose was 10 mm. The tests were performed under a displacement-controlled speed of 1.0 ± 0.2 mm min^{-1}. The data acquisition rate was 20 samples per second.

A 300 kN electromechanical MTS INSIGHT universal machine equipped with a 300 kN load cell calibrated at 100% was used for compression and In-plane shear (IPS) tests at room temperature. Compression tests were carried out following the ASTMD6641M-16 standard. The test machine was equipped with compression plates and fixture torque for clamping specimens was set at 11 Nm. To obtain the compressive modulus, one longitudinal strain gauge was placed in the middle of the specimen. The compression crosshead displacement rate was 1.3 mm min^{-1}, measured with a linear variable differential transformer (LVDT). The data acquisition frequency was 20 Hz.

In-plane shear (IPS) tests were performed according to EN 6031. The grip pressure holding the specimens was 10.3 MPa. To obtain the shear modulus and the maximum shear strain, in addition to the shear strength, one axial and one transversal strain gauge were used. The data acquisition frequency was 20 Hz. The test machine had been previously aligned following Nadcap procedures to achieve 8% maximum bending.

The glass transition temperature (T_g) was obtained using a DSC from TA Instruments, Model Q2000. The temperature range was 30°C - 250°C at a heating rate of 10°C min^{-1}. Aluminium pans were used for reference and samples. Measurements were taken with a continuous purge of nitrogen (99.999% purity) at a flow rate of 50 ml min^{-1}.

The thermal vacuum outgassing test was used to measure the total mass loss (TML). Note that, in the aerospace industry, the outgassing of materials must be less than 1% of TML. A TML lower than 5% is usually allowable for hygroscopic materials like CFRP or thermal foil [36]. Outgassing tests

were performed according to an internal procedure which is an adaptation of the ASTM E 1559 standard and consists of measuring the weight loss of the material after 24 hours at 125 °C under vacuum, and then measuring weight recovery after 24 hours in laboratory conditions.

The void content, which should be less than 1% for aerospace composites [35], and fibre volume fraction were measured following the EN2564:2018 (Method B) standard.

3 Results

In this section we present the result of implementing the Curing Cycles proposed in the previous section in the autoclave.

3.1 Optimized cure Cycle 1

Figure 5 shows the temperature evolution for 4 of the 11 thermocouples embedded within the 2 mm-thick panel during MRCC. All thermocouples strictly followed the same temperature–time curve and no temperature gradients or local temperature overshoots were observed.

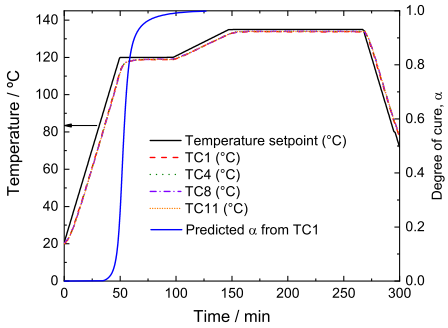

Fig. 5 The solid black line is the setpoint temperature of the autoclave corresponding to the MRCC. The dashed lines are the evolution of the temperature measured for a 2 mm thick panel with embedded thermocouples; only 4 thermocouples are shown to represent the behaviour of all. The blue solid line is the predicted evolution of the degree of cure calculated from the thermal history recorded by the TC1 thermocouple.

The measured temperature–time profile during the MRCC cycle was used to fuel the kinetic method, Equation 4, used to predict the evolution of the degree of cure using the kinetic parameters obtained in [24] (Figure 1): pre-exponential term and apparent activation energy. According to the prediction model's output (Figure 5), the maximum curing degree is reached before the second isotherm. The absence of thermal gradients (Figure 5) leads to an identical degree of cure throughout the composite panel, so a completely uniform cure progress is foreseen.

The full degree of cure in the prediction (Figure 5) marks the onset of the cooling ramp for the time-optimized Cycle **1**. Consequently, the duration of

Cycle **1** was reduced to 180 minutes (Figure 6) - versus 322 minutes for MRCC (Figure 5). Moreover, as we will point out in the discussion section, the glass transition temperature measured after cure Cycle **1** is 110.9°C, very similar to that obtained with the MRCC (111.7°C), so we can confirm that after Cycle **1**, the laminate is practically fully cured.

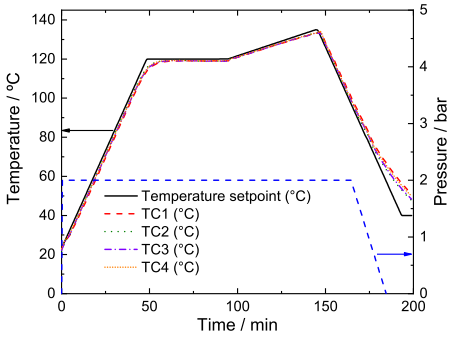

Fig. 6 The solid black line is the setpoint temperature of the autoclave corresponding to the cure Cycle **1**. The dashed lines are the evolution of the temperature measured for a 2 mm thick panel with embedded thermocouples.

Figure 6 shows the temperature recorded at different locations of the panel during the cure Cycle **1**. As expected, all recorded evolutions closely followed the setpoint temperature of the autoclave and no thermal gradients were observed.

3.2 Optimized cure Cycle 2

Cure Cycle **2** aimed at increasing the temperature ramps while controlling the rate of curing to avoid an excessive exothermal flow that could lead to undesirable local overheating. Therefore, the objective was to maintain the maximum curing rate peak close to that of the MRCC and Cycle **1** (0.0016 s^{-1}) because no overshoots had appeared in their measured cycles (Figures 5 and 6). The proposed curing Cycle **2** is shown in Figure 7: it starts with a fast heating ramp (10°C min^{-1}) which is maintained while the reaction rate is slow. When the reaction rate becomes significant, 120°C, a slower heating ramp (1.25°C min^{-1}) is established. When the transformation rate is relatively low, 125°C, a fast heating ramp of 10°C min^{-1} is set until a temperature of 150°C is reached. The last step is a dwell for 16.5 minutes at 150°C. The maximum curing rate of Cycle **2** is 0.0027 s^{-1} (40.7% more compared to MRCC and Cycle **1**), so an overshoot could not be fully discarded until testing had been carried out.

Cure cycle **2** was programmed in the control of the autoclave (represented by the dashed red line in Figure 8). The cooling ramp was set at 5°C min^{-1} to avoid warping in the panel. The measurement of the temperature during cure Cycle **2** (Figure 8) showed a good homogeneity (similar evolution for all

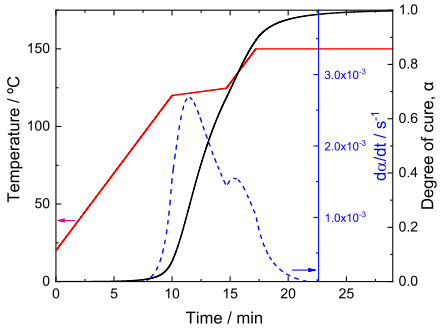

Fig. 7 The solid red line is the temperature program designed for the curing Cycle **2**. The solid black line and the dashed blue line are the predicted evolution of the curing degree and curing rate, respectively.

the thermocouples), however, the temperature in the panel did not reach the programmed heating ramp (10°C min^{-1}) due to the thermal inertia of the autoclave, resulting in a maximum curing rate of 0.0020 s^{-1}, instead of 0.0027 s^{-1}.

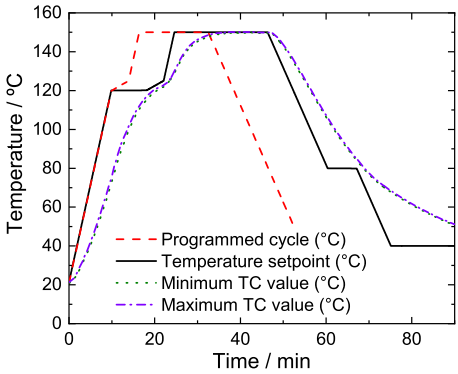

Fig. 8 Programmed cycle, autoclave setpoint, and measured temperature evolution for cure Cycle **2**. Thermocouples are placed close to each corner at the top of the CFRP panel.

In addition, the automatic autoclave self-regulation control, driven by safety criteria, introduced undesired segments into the thermal history (Figure 8). In fact, it introduced an isotherm segment at 120 °C for 10 minutes (solid black line). The short dwell at 80°C during the cooling ramp is due to the autoclave releasing the pressure. The real cycle took 90 minutes, while the prescribed one would have taken 53 minutes (Figure 8). In comparison to the MRCC, the real Cycle **2** represents a 72% reduction in curing time (from 322 to 90 minutes). The visual inspection of the cured panel revealed no distortions or other noticeable defects (e.g., matrix cracking, voids or microporosity).

The thermal history recorded in the autoclave (solid black line in Figure 9) was used to predict the evolution of the degree of curing (dotted black line in

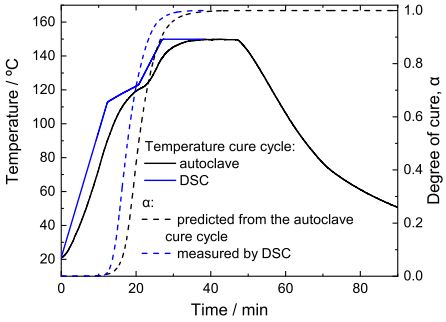

Fig. 9 Comparison between the thermal history (solid line) and degree of cure (dotted line) of the real cure cycle (black color), and the DSC measurement (blue). The degree of cure for the real thermal history is predicted, while the one for the DSC program is measured.

Figure 9). The predicted evolution indicates that the panel is fully cured after Cycle **2**.

To experimentally verify that the resin was fully cured, we programmed a thermal history in the DSC as similar as possible to that of the autoclave. In Figure 9 the solid blue line is the DSC temperature program, while the dashed blue line is the degree of cure determined from the DSC measurement. The DSC experiments shows that the laminate was fully cured in less than 40 minutes. Nevertheless, the DSC results and the prediction obtained from the autoclave cycle are shifted because the autclave thermal history is delayed with respect to the DSC temperature program. To better compare the results, in Figure 10, the reaction rate has been plotted as a function of temperature, rather than time. The predicted and measured curing rates are quite similar, although the peak for the autoclave cycle is slightly wider than that of the DSC due to the slower initial heating ramp.

Finally, as we will see below, the glass transition temperature measured is similar to that obtained with the MRCC, which confirms that almost complete curing has been achieved. Furthermore, the fact that the maximum curing temperature of the Cycle **2** (150°) is well above the maximum glass transition temperature (111.7°) ensures that the vitrification does not prevent the laminate from fully curing.

3.3 Mechanical and physical properties

Table 2 shows the mean, standard deviation, and relative variation with respect to the MRCC value of the properties specified in the test matrix (Table 1).

The higher the ILSS, compression, IPS, T_g and FVF parameters, the better the thermomechanical performance of the material. In contrast, the higher the TML and VC, the worse the composite material.

The interlaminar shear strength (ILSS) slightly decreased from the MRCC to Cycle **2**. For the latter cycle, the reduction reached 4% (Table 2). Compression and in-plane shear tests were performed for the MRCC and cure Cycle **1**. The ultimate compressive strength exhibited a relatively high dispersion,

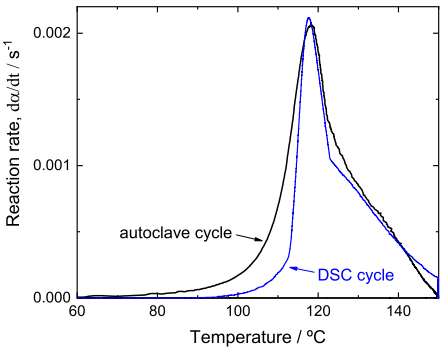

Fig. 10 Comparison between the reaction rate prediction for the autoclave cure cycle, and the reaction rate determined from the DSC signal.

and the average was 4.6% higher for Cycle 1. For the in-plane shear strength, practically identical results were obtained. The glass transition temperature decreased by 0.8 °C and 2.1 °C with respect to MRCC for curing Cycles **1** and **2**, respectively. Regarding the outgassing test, the total mass loss (TML) decreased with shorter curing cycles, with Cycle **2** exhibiting the minimum. The fibre volume fraction peaks for Cycle 1, and is 2% higher than for MRCC. Void content was below 1% for all curing cycles with Cycle **1** having the minimum average and Cycle **2** the maximum (see Table 2).

4 Discussion

For the VTC401 resin, a 38% and 72% reduction in curing time with respect to the manufacturer's recommended curing cycle was achieved following two optimized cycles. Certainly, these are high time reductions compared to those determined by existing optimization models (e.g., 33% for RTM6 epoxy resin [9], 19% [8] and 45% [10] for 3501-6). It should be noted, however, that the faster curing is associated to the diamine content of VTC401 which provides a greater margin for time improvement than traditional resins do [24]. The results of the mechanical tests show that for both optimized cycles, the relative reduction in properties is less than 4%. Moreover, the glass transition temperature decreased by as much as 2.1 °C for the fastest cycle. The fact that the glass transition temperatures of the laminates after the curing cycles **1** and **2** are similar to that of the MRCC, indicates that in all cases we practically reach a complete degree of cure. A TML percentage notably lower than 1% is obtained for all three cycles, while the most adverse value - void content - is also far below the 1% limit widely imposed in the aerospace sector. The results exemplify the potential of the isoconversional kinetic model to shorten curing cycles while, at the same time, assuring high mechanical performance.

The standard deviation values of the mechanical and physical properties are outstanding except for void content (50% worst case). The porosity in most composite panels is heterogeneous. Therefore, the void content is sensitive to

Table 2 Test matrix for the MRCC and cure cycles 1 and 2 (*does not apply to cure cycle 2)

Property		MRCC	Cure cycle **1**	Cure cycle **2**
Interlaminar shear strength (MPa)	Mean	66.8	65.9	64.1
	Standard deviation	1.7	1.4	1.6
	Relative deviation		-1.3%	-4.0%
Compression strength (MPa)	Mean	581	608	
	Standard deviation	64.7	50.9	
	Relative deviation		4.6%	
In-plane shear strength (MPa)	Mean	94.1	93.9	
	Standard deviation	0.84	0.74	
	Relative deviation		-0.21%	
Glass transition temperature (°C)	Mean	111.7	110.9	109.6
	Standard deviation	0.49	0.85	0.28
	Relative deviation		-0.7%	-1.9%
Total mass loss (%)	Mean	0.64	0.51	0.50
	Standard deviation	0.0007	0.059	0.0064
	Relative deviation		-20.3 %	-21.9%
Fibre volume fraction (%)	Mean	54.31	55.39	52.27
	Standard deviation	0.071	0.028	1.56
	Relative deviation		2.0 %	-3.8 %
Void content (%)	Mean	0.31	0.19	0.41
	Standard deviation	0.247	0.035	0.205
	Relative deviation		-38.7 %	-32.3 %

the local area in the panel from where the specimens are extracted. Although the specimens have been extracted from the same area for all the panels, this could be the main cause of the relatively high standard deviation in the void content values. Moreover, the cause for the slight dispersion of compressive strength (8.4% standard deviation) could be manufacturing variability. This type of test is highly sensitive to the parallelism between compression edges (0.03 mm according to the applied standard). Thus, a slight variation of this dimension in manufacturing leads to remarkably different values in testing.

The procedure used to determine cure Cycle **1** (monitoring the temperature during a prescribed cycle and using the actual thermal history to predict the evolution of the degree of cure) opens the door to optimising curing for components of arbitrary geometry and under arbitrary thermal programs. This means that the prediction method is universally applicable following this first approach. For example, if the dimensions of the composite part are increased remarkably (in-plane and/or thickness), customized time-reduced cycles different from those shown in the present study will be obtained. The reason

is that the thermal history recorded by the thermocouples (and with which the prediction model is powered) will be distinct. Thus, the presented findings are not limited to a specific CFRP flat panel 2 mm thick but can be extended to different thickness and geometries. Moreover, although this procedure entails manufacturing a first scrap part, the advantages achieved mean that in a production series, this loss will be rapidly outweighed.

Likewise, it has been shown that the model allows accurate predictions to be made for any temperature program without entering an experimental T–t profile; as evidenced with cure Cycle **2**. However, accurate results have been obtained with flat thin laminates and relatively small parts, where heat transfer does not play a relevant role because the thermal gradients are negligible and thus temperature is considered uniform through the thickness [37–39]. As a shortcoming to highlight, this second approach (imposing a theoretical temperature–time profile) will lead to inaccuracies in curing prediction when thermal inertia and/or overheating start to play a relevant role because the kinetic model is not coupled to a heat transfer analysis, as aforementioned. That is, heat released during curing is analysed but the heat accumulated due to the limited heat dissipation of the laminate is not. Therefore, the current methodology cannot evaluate whether the composite part will overheat during curing. Merging the current kinetic model with numerical modelling of the heat transfer problem could be done straightforwardly.

In addition, it should be noted that no limitations are anticipated when potentially applied to other thermosetting matrix systems, i.e., the curing time savings would be similar using a bismaleimide (BMI) or cyanate-esters (CT) matrix. In fact, the reaction mechanisms are equivalent to those of an epoxy resin used in the present study. Anyhow, firstly the kinetics of every particular resin system should be characterized correctly to determine its Arrhenius parameters and apparent activation energy as a function of the degree of cure.

5 Conclusions

In the present research, the feasibility of shortening curing cycles in an industrial environment has been demonstrated using a prediction method based on isoconversional kinetics. With the current approach, a total reduction in time of up to 72% has been achieved compared to the cure cycle recommended by the prepreg manufacturer. Several $300 \times 300 \times 2$ mm^3 carbon-epoxy VTC401/M55J flat panels were manufactured under different cure cycles, and resulted in a loss of mechanical (ILSS) and thermal properties (T_g) below 4% and 1.9%, respectively. In addition, in the worst case, we obtain a void content of 0.41% and an outgassing value of 0.64%, both of which are considerably lower than the 1% allowed by the aeronautic sector for these parameters. Therefore, the optimized cycles developed in this study could be used in the composite industry, enabling a reduction in production times without compromising material performance.

The proposed method has also shown that the transformation rate from the exothermic reaction during the curing process can also be predicted correctly. Therefore, not only has the maximum degree of cure in the shortest time been obtained, but the maximum transformation rate has also been controlled to constrain the heat flow from the exothermic reaction and avoid any detrimental effects (overheating).

Acknowledgments. This study was funded by the Generalitat de Catalunya under contract no. 2018DI0053 (Industrial Doctorate grant) and by the Spanish Agencia Estatal de Investigación through the project PID2021-126989OB-I00 /10.13039/501100011033/FEDER, UE. Daniel Sánchez-Rodríguez acknowledges the support received from the Beatriu de Pinós Programme and the Ministry of Research and Universities of the Government of Catalonia (Fellowship BP00069).

Conflict of Interest. There are no conflicts of interest to declare.

Authors' contributions. Data collection was performed by José Antonio González. Data analysis was performed by José Antonio González and Jordi Farjas. Experiment design and planning were performed by José Antonio González, Jordi Farjas, Norbert Blanco, Josep Costa and Marc Gascons. Kinetic Analysis and calculations were performed by Jordi Farjas and Daniel Sanchez-Rodriguez. José Antonio González wrote the manuscript. Scientific discussion and mansucript revision by José Antonio González, Jordi Farjas, Norbert Blanco, Josep Costa and Marc Gascons.

References

[1] Struzziero, G., Teuwen, J.J.E., Skordos, A.A.: Numerical optimisation of thermoset composites manufacturing processes: A review. Composites Part A: Applied Science and Manufacturing **124**, 105499 (2019)

[2] Ltd, S.C.M.: VTC401 Epoxy Component Prepreg, Product Data. (2018)

[3] Aleksendrić, D., Carlone, P., Ćirović, V.: Optimization of the temperature-time curve for the curing process of thermoset matrix composites. Applied Composite Materials **23**(5), 1047–1063 (2016)

[4] Nele, L., Caggiano, A., Teti, R.: Autoclave cycle optimization for high performance composite parts manufacturing. Procedia CIRP **57**, 241–246 (2016). Factories of the Future in the digital environment - Proceedings of the 49th CIRP Conference on Manufacturing Systems

[5] Yoon, J.-S., Kim, K., Seo, H.-S.: Computational modeling for cure process of carbon epoxy composite block. Composites Part B: Engineering **164**, 693–702 (2019)

[6] Agius, S.L., Joosten, M., Trippit, B., Wang, C.H., Hilditch, T.: Rapidly cured epoxy/anhydride composites: Effect of residual stress on laminate shear strength. Composites Part A: Applied Science and Manufacturing **90**, 125–136 (2016)

[7] Jouyandeh, M., Paran, S.M.R., Jannesari, A., Puglia, D., Saeb, M.R.: Protocol for nonisothermal cure analysis of thermoset composites. Progress in Organic Coatings **131**, 333–339 (2019)

[8] Tang, W., Xu, Y., Hui, X., Zhang, W.: Multi-objective optimization of curing profile for autoclave processed composites: Simultaneous control of curing time and process-induced defects. Polymers **14**(14) (2022)

[9] Dolkun, D., Zhu, W., Xu, Q., Ke, Y.: Optimization of cure profile for thick composite parts based on finite element analysis and genetic algorithm. Journal of Composite Materials **52**(28), 3885–3894 (2018)

[10] Yuan, Z., Tong, X., Yang, G., Yang, Z., Song, D., Li, S., Li, Y.: Curing cycle optimization for thick composite laminates using the multi-physics coupling model. Applied Composite Materials **27**(6), 839–860 (2020)

[11] Struzziero, G., Skordos, A.A.: Multi-objective optimisation of the cure of thick components. Composites Part A: Applied Science and Manufacturing **93**, 126–136 (2017)

[12] S. Hernández and F. Sket and C. González and J. Llorca: Optimization of curing cycle in carbon fiber-reinforced laminates: Void distribution and mechanical properties. Composites Science and Technology **85**, 73–82 (2013)

[13] Struzziero, G., Skordos, A.A.: Multi-objective optimization of resin infusion. Advanced Manufacturing: Polymer & Composites Science **5**(1), 17–28 (2019)

[14] Vyazovkin, S., Burnham, A.K., Criado, J.M., Pérez-Maqueda, L.A., Popescu, C., Sbirrazzuoli, N.: Ictac kinetics committee recommendations for performing kinetic computations on thermal analysis data. Thermochimica Acta **520**(1), 1–19 (2011)

[15] Vyazovkin, S., Sbirrazzuoli, N.: Isoconversional kinetic analysis of thermally stimulated processes in polymers. Macromolecular Rapid Communications **27**(18), 1515–1532 (2006)

[16] Wan, J., Li, C., Bu, Z.-Y., Xu, C.-J., Li, B.-G., Fan, H.: A comparative study of epoxy resin cured with a linear diamine and a branched polyamine. Chemical Engineering Journal **188**, 160–172 (2012)

[17] Stanko, M., Stommel, M.: Kinetic prediction of fast curing polyurethane resins by model-free isoconversional methods. Polymers **10**(7) (2018)

[18] Sbirrazzuoli, N.: Model-free isothermal and nonisothermal predictions using advanced isoconversional methods. Thermochimica Acta **697**, 178859 (2021)

[19] Hu, J., Shan, J., Zhao, J., Tong, Z.: Isothermal curing kinetics of a flame retardant epoxy resin containing dopo investigated by dsc and rheology. Thermochimica Acta **632**, 56–63 (2016)

[20] Budrugeac, P., Cucos, A., Dascălu, R., Paraschiv, C., Mitrea, S., Sbarcea, B.-G.: The use of thermal analysis methods for predicting the thermal endurance of an epoxy resin used as electrical insulator. Journal of Thermal Analysis and Calorimetry **146**(4), 1791–1801 (2021)

[21] Kyriakou-Tziamtzi, C., Vlachopoulos, A., Zamboulis, A., Bikiaris, D.N., Achilias, D.S., Chrissafis, K.: Kinetic evaluation of the crosslinking of a low-temperature cured biobased epoxy-diamine structure. Progress in Organic Coatings **174**, 107285 (2023)

[22] Sanchez-Rodriguez, D., Zaidi, S., Jahani, Y., Ruiz de Luzuriaga, A., Rekondo, A., Maimi, P., Farjas, J., Costa, J.: Processability and reprocessability maps for vitrimers considering thermal degradation and thermal gradients. Polymer Degradation and Stability **217**, 110543 (2023)

[23] Jamali Moghadam Siahkali, M., Guigo, N., Sbirrazzuoli, N.: Cross-Linking Mechanisms of a Rigid Plant Oil-Based Thermoset from Furfural-Derived Cyclobutane. Macromolecules (2022)

[24] Jose Antonio González Ruiz and Jordi Farjas and Norbert Blanco and Josep Costa and Marc Gascons: Assessment of unexplored isoconversional methods to predict epoxy-based composite curing under arbitrary thermal histories. Journal of Reinforced Plastics and Composites **42**(19-20), 1067–1074 (2023)

[25] Vyazovkin, S.: Evaluation of activation energy of thermally stimulated solid-state reactions under arbitrary variation of temperature. Journal of Computational Chemistry **18**(3), 393–402 (1997)

[26] Farjas, J., Roura, P.: Isoconversional analysis of solid state transformations. A critical review. Part II. Complex transformations. Journal of Thermal Analysis and Calorimetry **105**(3), 767–773 (2011)

[27] Vyazovkin, S., Burnham, A.K., Favergeon, L., Koga, N., Moukhina, E., Pérez-Maqueda, L.A., Sbirrazzuoli, N.: ICTAC Kinetics Committee recommendations for analysis of multi-step kinetics. Thermochimica Acta,

178597 (2020)

[28] Dunne, R.C., Sitaraman, S.K., Luo, S., Rao, Y., Wong, C.P., Estes, W.E., Gonzalez, C.G., Coburn, J.C., Periyasamy, M.: Investigation of the curing behavior of a novel epoxy photo-dielectric dry film (ViaLux™81) for high density interconnect applications. Journal of Applied Polymer Science **78**(2), 430–437 (2000)

[29] Granado, L., Tavernier, R., Foyer, G., David, G., Caillol, S.: Comparative curing kinetics study of high char yield formaldehyde- and terephthalaldehyde-phenolic thermosets. Thermochimica Acta **667**, 42–49 (2018)

[30] Wuzella, G., Mahendran, A.R., Beuc, C., Lammer, H.: Isoconversional cure kinetics of a novel thermosetting resin based on linseed oil. Journal of Thermal Analysis and Calorimetry **142**(2), 1055–1071 (2020)

[31] Vafayan, M., Hosain Beheshty, M., Ghoreishy, M.H.R., Abedini, H.: Advanced integral isoconversional analysis for evaluating and predicting the kinetic parameters of the curing reaction of epoxy prepreg. Thermochimica Acta **557**, 37–43 (2013)

[32] Farjas, J., Roura, P.: Isoconversional analysis of solid-state transformations. Journal of Thermal Analysis and Calorimetry **109**(1), 183–191 (2012)

[33] Rasi, S., Roura-Grabulosa, P., Farjas, J.: Application of thermal analysis and kinetic predictions to ybco films prepared by chemical solution deposition methods. Journal of Thermal Analysis and Calorimetry **142**(5), 2077–2086 (2020)

[34] Rajanish, M., Nanjundaradhya, N.V., Sharma, R.S.: An investigation on ilss properties of unidirectional glass fibre / alumina nanoparticles filled epoxy nanocomposite at different angles of fibre orientations. Procedia Materials Science **10**, 555–562 (2015). 2nd International Conference on Nanomaterials and Technologies (CNT 2014)

[35] Anandan, S., Dhaliwal, G.S., Samaranayake, V.A., Chandrashekhara, K., Berkel, T.R., Pfitzinger, D.: Influence of cure conditions on out-of-autoclave bismaleimide composite laminates. Journal of Applied Polymer Science **133**(38) (2016)

[36] Zhang, G., Luo, L., Lin, T., Zhang, B., Wang, H., Qu, Y., Meng, B.: Multi-objective optimisation of curing cycle of thick aramid fibre/epoxy composite laminates. Polymers **13**(23) (2021)

[37] Lahuerta, F., Nijssen, R.: Influence of internal temperature development

during manufacturing on thick laminates compression fatigue properties. IOP Conference Series: Materials Science and Engineering **139**(1), 012028 (2016)

[38] Qiao, W., Yao, W.: Modelling of process-induced deformation for composite parts considering tool-part interaction. Materials **13**(20) (2020)

[39] Dolkun, D., Wang, H., Wang, H., Ke, Y.: Influence of large framed mold placement in autoclave on heating performance. Applied Composite Materials **27**(6), 811–837 (2020)